Integrated Open-Source Software for Multiscale Electrophysiology

Konstantinos Nasiotis[a,*], Martin Cousineau[a], François Tadel[b], Adrien Peyrache[a], Richard M. Leahy[c], Christopher C. Pack[a], Sylvain Baillet[a]

[a] Montreal Neurological Institute, McGill University, Montreal, QC, Canada

[b] Grenoble Institute of Neuroscience, Grenoble, France

[c] Signal & Image Processing Institute, University of Southern California, Los Angeles, USA

[*] Correspondence: konstantinos.nasiotis@mail.mcgill.ca

Abstract

The methods for electrophysiology in neuroscience have evolved tremendously over the recent years with a growing emphasis on dense-array signal recordings. Such increased complexity and augmented wealth in the volume of data recorded, have not been accompanied by efforts to streamline and facilitate access to processing methods, which too are susceptible to grow in sophistication. Moreover, unsuccessful attempts to reproduce peer-reviewed publications indicate a problem of transparency in science. This growing problem could be tackled by unrestricted access to methods that promote research transparency and data sharing, ensuring the reproducibility of published results.

Here, we provide a free, extensive, open-source software that provides data-analysis, data-management and multi-modality integration solutions for invasive neurophysiology. Users can perform their entire analysis through a user-friendly environment without the need of programming skills, in a tractable (logged) way. This work contributes to open-science, analysis standardization, transparency and reproducibility in invasive neurophysiology.

Introduction

Invasive electrode recordings are a unique source of in-vitro and in-vivo neurophysiological data at high resolution in both space and time, recorded in relation to complex animal and human behavior. The complexity of this kind of data has increased in recent years, with the advent of increasingly dense multi-channel and multi-site electrode arrays. This evolution provides exciting opportunities to explore the relationship between local events, such as action potentials, and more global dynamics at the systems level, such as fluctuations in oscillatory network activity. At the same time, these multiscale explorations require different analytical methods from those traditionally used in the field.

Challenges in exploring high-dimensional spatio-temporal data sets are not specific to electrophysiology: they occur frequently in neuroimaging data, as scanners produce increasingly large volumes of data, which are often shared across multiple groups or research centres. In response, the brain imaging community has made significant strides in developing shared software platforms to harmonize analytical methods and to facilitate data sharing (Abraham et al., 2014; Gorgolewski et al., 2011; Gramfort et al., 2013, 2014; Hanke et al., 2009; Tadel et al., 2011). Indeed, free, open-source software toolkits have been critical for facilitating training and augmenting research productivity. This approach has transferred to the field of scalp electrophysiology (Baillet et al., 2011), but as of yet it has not found widespread use in invasive neurophysiology (IN). Software tools do exist for specific segments of the IN data workflow, such as for spike detection and sorting and time-series analysis (Fee et al., 1996; Hazan et al., 2006; Hill et al., 2011; Mitra and Bokil, 2007; Oostenveld et al., 2011; Pachitariu et al., 2016; Quiroga et al., 2004), but they remain relatively specialized, some with limited support and documentation and most with restricted interoperability with other tools.

While we acknowledge significant efforts in harmonizing data formats for electrophysiology (Stead and Halford, 2016; Teeters et al., 2015; Neuroshare - http://neuroshare.sourceforge.net/index.shtml) , it does seem that this field lags behind others in meeting the demands of recommended practices for data management and transparency (Gorgolewski and Poldrack, 2016; Larson and Moser, 2017). In this regard, well-supported software tools are required to produce analytical workflows that are validated, well documented and reproducible. Important components include data organization, review and quality control, verified implementations of signal extraction and decomposition methods, solutions for advanced visualization registered to anatomy, and sound approaches to machine learning and statistical inference. As in the brain imaging field, such tools would facilitate the reproducibility of published results and the dissemination of methods within and between research groups. They would also save considerable time and resources currently required to re-code published methods. In addition, re-coding presents challenges in code verification relative to a published method, raising possible concerns about the validity of the end results and limiting the long-term value of the effort.

Here we deploy and share open-source software (called *Invasive Neurophysiology*-Brainstorm, or *IN-Brainstorm*) that integrates multiple aspects of data analysis for most modalities and signal types for basic electrophysiology: from single cells to distributed channel arrays, from spiking events to local field potentials, from ongoing recordings to event-related responses, and from in

76   vitro preparations to free-behaving models. We also emphasize the importance of an extensive
77   graphical interface for user-friendly access to advanced analytical methods, of flexible scripting
78   features for high-performance computing, and of traceable code execution. The proposed tool is
79   accompanied by extensive online documentation and support from a user community web
80   forum.

81   This free application builds on the foundations of the *Brainstorm* platform (Tadel et al., 2011),
82   which is well-established (21,000 user accounts), free open-source software for
83   magnetoencephalography (MEG) and electroencephalography (EEG). Brainstorm can integrate
84   multimodal data volumes in addition to scalp electrophysiology e.g., magnetic resonance imaging
85   (MRI), CT-scans and functional near-infrared spectroscopy (fNIRS). It also features advanced
86   source modeling for electrophysiological signals.

87   The IN-Brainstorm application provides a comprehensive suite that interoperates with other,
88   more specific and constantly evolving IN tools available from the open-source community e.g.,
89   for performing spike sorting. The end result is a unique and expansive software toolkit that
90   bridges across recording scales and data modalities, registers invasive neurophysiology with
91   structural anatomy data, and thereby delivers a unifying analytical environment to the
92   neurophysiology research community.

93

Results

The IN-Brainstorm functionalities described here offer comprehensive solutions for data importation and analysis, including spike-sorting, extraction of local field potentials, and correlations among these measures across multiple channels. Importantly, thanks to an intuitive graphical user interface, no programming skills are required for accessing and using the advanced methods available, including for assembling and sharing advanced data analysis pipelines. A summary of these software features is provided in Table 1, and a schematic of the workflow enabled by the toolbox is shown in FIGURE 1.

The bedrock of the present developments is the Brainstorm platform. Brainstorm (Tadel et al., 2011) is written in Matlab (Matlab2008a and higher) and Java. It is therefore independent of the operating system (Windows, MacOS and Linux). Community code management is via GitHub. Users without access to a Matlab license can use a fully executable version of the application compiled for the above operating systems. Extensive documentation is freely available online, with specialized tutorials, datasets and videos (https://neuroimage.usc.edu/brainstorm/e-phys/Introduction).

In the following sections, we describe a broad spectrum of analysis options for multiscale electrophysiology that are enabled by IN-Brainstorm and illustrate these features with the processing of an example raw data file.

1. Importing, reviewing and pre-processing raw data

1.1. Raw data importation

Data to be analyzed must first be imported into the software. Brainstorm can read raw electrophysiology data from 80 different file formats. We have added new data formats specific to single- and multi-unit electrophysiology, including Plexon (.plx and .pl2), Blackrock (.nsX), Ripple (.nsX), Intan (.rhd), Tucker Davis Technologies, and Neurodata Without Borders (.nwb). New formats can be added on demand. Raw data can also be read directly from ASCII and basic binary data formats, with header file parameters easily specified from a GUI.

1.2. Data review

Raw files of continuous data from chronic preparations can be voluminous due to hours-long durations, tens of kilo-Hertz sampling rate and simultaneous recording from multi-channel electrode arrays. Hence loading such large raw files at once into computer memory can be impractical. For this reason, we have implemented efficient data review solutions that load portions of the data on the fly, depending on the visualization parameters set by the user (e.g., virtual page length, selection of a subset of channels or montages for review, keyboard and mouse shortcuts for navigating and marking events).

Task events (e.g., stimulus types and presentation times, behavioral responses) and ancillary recordings (electrooculograms, electrocardiogram, eye and body movements, video recordings of behaviour, etc.) are readily registered to the electrophysiological data in IN-Brainstorm, for

132   multimodal data review, quality control and event-related processing. We emphasize that when
133   a raw file is reviewed, the physical data is not duplicated as a Brainstorm file. Instead, the header
134   of the original data file is automatically parsed to extract metadata, such as channel parameters,
135   sampling rate, time stamps, event codes, etc.

136   Figure 2 (left) shows an example of IN-Brainstorm display for data review, including sub-menus
137   for displaying and navigating through files and events. The right panel shows an example of raw
138   data collected with a Plexon MAP system and a 32-channel linear electrode implanted in cortical
139   areas MT and MST of a non-human primate. The animal maintained fixation during the
140   presentation of a motion stimulus comprising of dots that translated in 8 different directions.

141   The red line in the figure shows the time of a *Stim On* event, extracted from the data. Spikes
142   detected online (labelled as *Spikes Channel*) were extracted directly from the raw file contents
143   by IN-Brainstorm, with automatic registration to the data time series.

144   The bottom right panel of Figure 2 shows a selection of 4 channels temporally aligned with the
145   top figure. The spikes from a neuron that was isolated on the first electrode are marked with
146   green circles at the top of the full time-series displayed in the top panel. Users can browse the
147   raw traces using point-and-click GUI and a series of keyboard shortcuts. On-the-fly bandpass and
148   notch filtering can be applied to the signals.

149   ## 1.3. Quality control & data pre-processing
150   Starting from the kind of raw data shown in Figure 2, users can easily navigate through the
151   recordings and experimental trials and events for quality control. Data segments, channels and
152   entire trials can be marked as "bad" and excluded from further analyses using automatic
153   processes or based on user evaluations.

154   The IN-Brainstorm pre-processing toolkit features solutions for adjustments of recording
155   baseline, data resampling and frequency filtering (with linear phase filters). Additionally,
156   detection and attenuation of artifacts (e.g., heartbeats, eye and body movements, stimulation
157   and juice artifacts) can be achieved with principal (Uusitalo and Ilmoniemi, 1997) or independent
158   component analysis (Bell and Sejnowski, 1995; Cardoso, 1999). Finally, combining sensor data
159   with the actual geometry of the recording array(s) enables many 2-D and 3-D visualization
160   possibilities for time-series and realistic topographical plots, as illustrated further below.

161   ## 2.   Spike detection and spike sorting
162   Following the importation and preprocessing of data, IN data is often processed to extract spiking
163   events from single or multiple neurons. This entails detecting spike occurrences and classifying
164   these events according to their respective neural sources (Quiroga, 2007). Most data acquisition
165   systems feature online spike detection and sorting. These online events can be imported directly
166   into IN-Brainstorm with the corresponding raw recordings. Yet, usual IN practice is to refine spike
167   classification with a two-step procedure consisting of 1) unsupervised clustering, which
168   automatically assigns each spike to a neural source based on waveform features, then 2)
169   supervised clustering, which requires manual reviewing and editing of the labels from
170   unsupervised clustering and the elimination of spurious spike events.

171 For IN-Brainstorm, we have enabled the direct interoperability with a selection of existing and
172 openly-available spike-sorting toolkits: *Waveclus* (Quiroga et al., 2004), *UltraMegaSort2000* (Fee
173 et al., 1996; Hill et al., 2011) and *Kilosort* (Pachitariu et al., 2016). Those packages can be
174 downloaded and installed automatically, in a completely transparent procedure. Sequentially,
175 these tools are called by and interact with IN-Brainstorm without programming interventions
176 from users.

2.1. Unsupervised spike sorting

178 Figure 3 (left) shows IN-Brainstorms' GUI for unsupervised spike-sorting. Raw files are dragged
179 and dropped into the GUI process box before a spike-sorting tool is selected from the IN-
180 Brainstorm toolkit. Next, spike events are detected on each electrode and classified according to
181 their putative neuronal generators.

182 The unsupervised spike events produced overwrite the online counterparts that were detected
183 during data acquisition. The output of the spike-sorting process (Figure 3 Box 1) is automatically
184 registered to and accessible from the IN-Brainstorm database and linked to the corresponding
185 raw file. The spike events are labelled in a principled manner (per channel and source cell number
186 – Figure 3 Box 2).

2.2. Supervised spike sorting

188 As *WaveClus* and *UltraMegaSort2000* have built-in supervised spike sorting graphical user
189 interfaces, we synchronized their GUIs with IN-Brainstorm's. For *Kilosort*, we developed specific
190 GUI bridges via *Klusters* (Hazan et al., 2006). The user-selected supervised clustering tool is called
191 from Brainstorm's main window after an unsupervised spike-sorted file is selected (Figure 4A).
192 The user then switches to the GUI of the selected supervised spike clustering tool (Figure 4 B-D).
193 Once supervised spike clustering is complete, the spike events are updated accordingly and
194 registered into the software's file system. Double-clicking on the link to the raw data file lets the
195 user review the updated spike events along with the raw electrophysiological traces as shown in
196 Figure 2 (Right).

197 Spike events and categories from other spike-sorting tools can be readily imported as Brainstorm
198 events, following the procedure described in the online documentation
199 (https://neuroimage.usc.edu/brainstorm/e-phys/ConvertToBrainstormEvents).

3. Extraction of local field potentials

201 In addition to spiking activity, IN recordings yield local field potentials (LFPs), which provide direct
202 measures of the summed post-synaptic electrical activity in the vicinity of recording electrodes
203 (Legatt et al., 1980). These can be useful as a complement to spiking activity or a surrogate for
204 some aspects of neural activity (e.g.,(Mineault et al., 2013)), provided that LFP traces can reliably
205 be filtered and separated from spike waveforms (Zanos et al., 2011).

206 Figure 5A shows the IN-Brainstorm's GUI for extracting LFP traces from raw recordings. The
207 application features efficient tools to remove spike traces (Zanos et al., 2011), to perform anti-
208 aliasing bandpass filtering and to down-sample the raw data. The de-spiking method proposed

209 by Zanos et al. (2011) increases the accuracy of subsequent spike-field coherence measures and
210 of spike-triggered average signals.

211 The resulting LFP traces and experimental events are automatically registered in IN-Brainstorm's
212 data repository for further review and analysis with a vast library of tools and pipelines – as
213 described below – or for easy exportation to other software or plain files.

214 LFP extraction produces a new IN-Brainstorm down-sampled time-series binary file (Figure 5B)
215 with all the corresponding metadata, such as channel description (e.g., electrode labels and
216 locations), and spike and experimental events. This file is easily sharable among researchers since
217 its size is typically ~20-30 times smaller than the original raw file. Figure 5C shows a segment of
218 the LFP file created.

4.   Epoching

220 Once the relevant neural signals (LFPs and spikes) have been extracted from the raw data, they
221 can be divided according to experimental epochs. Epochs are typically comprised of experimental
222 trials, with the time window selection defined around a stimulation or behavioral event of
223 interest. These can be imported directly into the IN-Brainstorm file system.

224 To illustrate these functions, we make use of the example visual cortex recording described
225 previously (Figure 2). The experiment involved presentations of moving stimuli while the animal
226 maintained fixation; we defined the relevant epochs as segments of [-500, 1000] ms around the
227 onset of each visual stimulus (Figure 6 Left). In total we considered 8 different directions of the
228 visual stimulus moving pattern; each stimulus condition was repeated 4 times (one condition was
229 repeated for 96 trials for usage in the raster plot, and noise correlation functions). Imported trials
230 to the database are shown in (Figure 6 – Right).

231 The following analysis steps can then be applied on the epoched trials.

5.   Analysis of individual LFP signals

233 LFP traces can be analyzed using Brainstorm's extensive library originally developed for EEG and
234 MEG research (Tadel et al., 2011). We show in Table 1 a list of the main data processing categories
235 that are available for LFP analysis. There is extensive online documentation, accompanied by data
236 files, that describes in detail the methods and practices of LFP signal analysis
237 (http://neuroimage.usc.edu/brainstorm).

238 We briefly provide below a few examples of these functions and their implementation in IN-
239 Brainstorm.

240

5.1. Time-frequency decompositions

242 Having extracted the LFP signal and defined an appropriate analysis epoch, one can compute the
243 LFP power at different frequencies and at different times relative to a stimulus event. Such

244 information is often used to infer stimulus selectivity, anatomical sources of input, and other
245 factors that are not necessarily apparent in spiking activity (Buzsáki, 2006; Fries et al., 2008;
246 Pesaran et al., 2002; Wilke et al., 2006; Womelsdorf et al., 2006).

247 IN-Brainstorm provides functionality for spectral and time-frequency decompositions, which can
248 be derived using power spectrum density estimates, Hilbert or wavelet transforms. An example
249 time-frequency decomposition (wavelet) is shown in Figure 7A for the example LFP data
250 corresponding to a single stimulus condition and epoch that shows a strong beta response after
251 stimulation. The wavelet decomposition was z-scored with respect to a pre-stimulus baseline [-
252 500:-100] ms.

253

254 ### 5.2. LFP-LFP signal analysis
255 LFP signals from multichannel recordings can be analyzed to detect occurrences of various forms
256 of signal similarities in the time or frequency domain. These measures are often interpreted as
257 representing functional connectivity between different sites (Fries, 2005; Fries et al., 2002, 2008;
258 Womelsdorf et al., 2006). IN-Brainstorm provides support for widely-used measures based on
259 amplitude or phase statistics as indicators of possible interregional brain interactions (coherence,
260 phase-locking values, bandlimited amplitude envelope correlations, phase-transfer entropy) and
261 parametric models (estimates of time- or frequency-domain Granger causality). Advanced
262 measures of interdependence between oscillatory components of polyrhythmic brain activity can
263 be derived with phase-amplitude coupling (PAC) estimation tools (Canolty et al., 2006, Samiee
264 and Baillet, 2017). An example estimation of coherence among all combinations of electrodes is
265 shown in Figure 7B for a single stimulus condition and epoch. The bimodal pattern that emerges
266 (high coherence among some channels and low coherence among others) is an indication of the
267 transition of the linear probe across neighboring cortical areas, from MT (electrodes 1:13) to MST
268 (14:32).

269

270 ## 6. Analysis of individual neuron spiking activity

271 Spikes are registered in IN-Brainstorm as events; the corresponding features are 1) the time of
272 occurrence and 2) a label for distinguishing between neuronal sources. We provide several
273 features for visualization of epoched spiking data.

274 ### 6.1. Raster plots
275 Raster plots are routinely used to visualize the relations between neuronal firing and a stimulus
276 event or a behavioral response. The spike occurrences in each trial and from each neuron are
277 binned over user-defined time epochs and converted into firing rates (spikes/second).

278 We provide two methods for visualizing spiking activity with IN-Brainstorm:

279 The first method shows the spiking data as trial vs. time bins for each neuron. Raster plots of
280 spiking rates are displayed after interactive selection of the cell to be reviewed. Figure 8A shows
281 the raster plot of the first neuron detected from contact AD01, with 10-ms binning. The trial

282 average of the neuron's firing rate from 96 trials of a single condition revealed a stimulus-onset-
283 to-maximum-firing latency of about 150 ms.

284 The second method is embedded within the topographical plots section as shown below.

6.2 Tuning curves
286 Tuning curves capture the relationship between an experimental variable (e.g., the orientation
287 of a visual stimulus) and a scalar measure of neural activity (e.g., a single neuron's trial-averaged
288 firing rate).

289 Tuning curves are readily produced from continuous data files that contain the event markers of
290 interest to the study. Tuning curves are displayed with IN-Brainstorm after manual assignment
291 of the order of the experimental conditions (x-axis), the selection of the neurons to be displayed,
292 and the selection of the time window of interest for reporting spiking activity. A separate tuning
293 curve figure is produced for each neuron selected.

294 We selected the events and individual neurons previously identified from spike sorting via IN-
295 Brainstorm's GUI. Figure 8B shows the tuning curves of one example neuron (labeled as "*Spikes*
296 *Channel AD07 |1|*") for the 8 different conditions (Stim On -3/4 pi, Stim On -2/4 pi etc.) of the
297 motion stimuli. The tuning curve shows the preference of this neuron for stimuli moving in the
298 right direction (*Stim On 0* condition).

299

6.3 Topographical plots
301 When multichannel recording devices are used, neurophysiology data can be shown as
302 topographically registered to structural anatomy. IN-Brainstorm can show neuronal firing at the
303 3-D locations of the recording probes/arrays. To illustrate this feature, we used a separate
304 dataset that was collected from two 96-channel Utah arrays and one 32-linear probe (Krause et
305 al., 2017). A structural T1-weighted MRI volume was acquired preoperatively. The head and brain
306 surface envelopes were segmented with Freesurfer (Fischl et al., 2001) and directly imported in
307 IN-Brainstorm. The electrode contact locations were co-registered to the 3-D anatomical volume
308 by specifying the distance of the electrodes along the probe and locating the tip of the probe and
309 the entry point through the skull, using Brainstorm's MRI volume viewer.

310 Neuronal firing was binned in 10-ms segments and displayed on the animal's anatomy as shown
311 in Figure 9A (a single bin is displayed in the figure). This figure shows IN-Brainstorm's ability to
312 overlay the segmented cortical surface, MRI orthogonal slices, the implanted devices with actual
313 geometry, and color-coded displays of raw or processed electrophysiology data (here
314 instantaneous firing rates). Figure 9B shows a zoomed-in version of Figure 9A over the Utah array
315 implanted in the prefrontal cortex.

316

7. Spike-spike analysis: Noise correlations

While tuning curves capture neuronal sensitivity to stimulus properties, the fidelity of a population code is thought to be limited by noise that is common across neurons (Zohary et al., 1994); for example, neurons would be noise correlated if for each stimulus their activities are correlated (Eyherabide and Samengo, 2013). Such noise correlations are typically quantified as the Pearson correlation coefficient between the firing rates of two neurons across trials. Such correlations strongly influence the accuracy of population coding (Abbott and Dayan, 1999; Averbeck et al., 2006; Liu et al., 2016; Panzeri et al., 1999; Sompolinsky et al., 2001).

Noise correlation statistics are displayed with IN-Brainstorm from the correlation of the spike trains that each neuron elicited within a given epoch, for all neuronal combinations. The end result is a *nxn* matrix (with *n* the number of unique neurons that produced spikes during the selected trials) that shows noise correlation estimates between the selected neurons.

Figure 8C shows the noise correlation profile across the 32-channel array of the example dataset, for 53 unique neurons that elicited spikes across all trials at the 8 conditions of presentation of the moving stimulus in the original data set from Figure 2. Spikes included in the correlation computations were selected in the [0,300]-ms time range of each trial.

The computed noise correlation showed 2 pairs of neurons with abnormally high noise correlation (above 0.8). After further inspection, it was revealed that this was due to the fact that the spike-sorter that was used was not taking into account the relative position of the electrodes, and the same neurons were picked up from neighbouring channels:

Neurons: AD01 |1| - AD02|2| and AD08 |1| - AD09 |1| were the same neuron.

8. Spike-LFP analysis

Spikes are local events, reflecting outputs from individual neurons. LFPs in contrast can capture activity over regions, including subthreshold post-synaptic activity, and therefore reflect the state of a broader network (Cui et al., 2016). There is considerable interest in relating the two types of signals for estimating the dependence of spiking activity on the broader context in which the neuron is embedded.

8.1. Spike-field coherence

Spike-field coherence (SFC) estimates the consistency between the time occurrence of spike trains and the phase of co-localized LFP cycles as a function of frequency (Arce-McShane et al., 2018). SFC can also be used to evaluate synchronized activity between distant brain regions, as a marker of neuronal communication (Fries, 2005; Gregoriou et al., 2009; Liebe et al., 2012; Singer, 1999; Womelsdorf et al., 2007). IN-Brainstorm features the spike-field coherence estimator proposed by Fries et al. (2001). The user can derive SFC estimates for each GUI-selected neuron, for all electrodes and frequencies of interest.

Figure 8D shows SFC up to 60 Hz between a single neuron detected at channel AD07 of the example data set and the LFP traces at all the 32 channels of the probe. The time window selected

354 around the spiking events was [-150, 150] ms. The horizontal white line indicates the electrode
355 where the neuron was detected.

356

8.2. Spike-triggered average of the LFP

358 Spike-triggered averaging (STA) of the LFP reveals how neuronal spiking is related to the dynamics
359 of proximal or distant LFPs (Jin et al., 2008; Nauhaus et al., 2009; Ray and Maunsell, 2011). STA
360 proceeds with trial averaging of LFP traces time-locked to a designated neuron's spike events,
361 followed by normalization with the total spike count.

362 Analogous to spike-field coherence, STA is computed over a user-selected time window around
363 each spiking event. STA scores are per neuron, showcasing the average LFP amplitude around
364 the occurrence of the spikes of each neuron. STA can be visualized on topological 2-D
365 representations of the recording array, to reveal time-locked associations between neuronal
366 spiking activity and local or remote LFP recordings.

367 Figure 8E shows the STA time-locked to the firing of the first neuron detected by electrode AD01
368 across trials and conditions. The topographical 2-D plot is produced with IN-Brainstorm using
369 multidimensional scaling of the actual 3-D location and geometry of the implanted probe. The
370 LFP epoch around spike event was [-150,150] ms.

9. Statistical inference and machine learning

372 Once measures have been extracted from spiking or LFP data, tools to conduct inferential
373 statistical analysis in the multiple dimensions of electrophysiological data (space, time,
374 frequency, connectivity) are available from Brainstorm's library.

375 Parametric (one- and two-sample tests) and nonparametric permutation tests, descriptive and
376 distribution statistics from histograms (Q-Q plot and Shapiro-Wilk test for data normality) are
377 available. Here too, the software architecture emphasises interoperability with other toolkits, for
378 expanded resources. For instance, multidimensional and nonparametric cluster statistics can be
379 run on LFP and time-frequency data, from Brainstorm, via calls to FieldTrip (Oostenveld et al.,
380 2011).

381 In addition, statistical learning tools for decoding and multivariate pattern analysis (MVPA) are
382 also available (see e.g., Cichy et al., 2014). The Brainstorm library also includes support vector
383 machine (SVM) and linear discriminant analysis (LDA) classification of LFP time series based on
384 experimental events and conditions.

385

386

387

10. Additional features

10.1 Processing power

Hardware acceleration in the processing of long recordings is enabled by Matlab's standard parallel computing (e.g., multi-core) features, which are controlled directly from Brainstorm's GUI. Flexible management of memory resources is also accessible to users, with the specification of the amount of RAM allocated to data manipulations while executing the LFP extraction process.

10.2 Data management

Generally speaking, formal data management plans are seldom adopted by electrophysiology labs. Instead, the handling of data is typically project-based, with trainees managing their individual data collection and analyses until publication. When they move on to another project or to the next step of their career, they frequently leave data, analysis pipelines and results behind, with minimal documented organization for sustainability and knowledge transfer. This limits the long-term value of data and negatively impacts the reproducibility and verification of research results (Baker, 2016). Brainstorm has tools to improve and facilitate data management: data is hierarchically organized by Studies, followed by Subjects/Samples and (experimental) Conditions, which point to data elements such as links to raw data files, single-trial epochs, sample statistics, and other derivatives: power spectra, wavelet decompositions, measures of cross-frequency coupling and inter-regional connectivity, etc. As with all features in the application, user interactions with Brainstorm's data organization are facilitated both by the application's GUI and direct access via scriptable functions using Matlab code.

Another important aspect of Brainstorm is its capacity for importing entire data repositories at once, with associated metadata, when those datasets are organized according to the emergent Brain Imaging Data Structure (BIDS). Originally driven by the neuroimaging community, BIDS is a grassroots effort to harmonize data organization and documentation (Gorgolewski et al., 2016). BIDS has recently been extended to MEG electrophysiology (Niso et al., 2018) and is presently integrating EEG (Pernet et al.), and invasive neurophysiology (Holdgraf et al.).

10.3 Batch processing

The software has a specific GUI for assembling data processing pipelines in an intuitive manner, choosing elementary processes from the (IN-)Brainstorm library and assembling them together into a logical progression along the workflow. These pipelines enable the reproduction of any data workflow with a click of a button. They can also be shared in Matlab format with collaborators or the entire user community. The Matlab code for pipelines can also be generated automatically by Brainstorm e.g., for execution in headless (no GUI) mode on high-performance computing servers and cloud resources.

Discussion

426

427 We provide a free, extensive open-source software application for invasive electrophysiology. IN-
428 Brainstorm is built on the foundations of Brainstorm, which was originally designed for human
429 multimodal electrophysiology and imaging. IN-Brainstorm supports multiple data formats of raw
430 signals from a variety of acquisition systems. The recorded traces and their LFP versions can be
431 reviewed, quality-controlled and processed within a unique analytical environment, with easy
432 GUI interactions, rich visualization, intuitive pipeline editing for scripting and sharing. We have
433 built bridges for IN-Brainstorm to interoperate seamlessly with established, free spike-sorting
434 tools.

435 A specific emphasis was put on providing versatile solutions for multidimensional data
436 visualization, including 2-D and 3-D topographical plots registered to structural anatomy from co-
437 registered MRI data. Source modeling of array data is also available using boundary element
438 modeling of head and brain tissues (Gramfort et al., 2010; Kybic et al., 2005) and a variety of
439 source modeling techniques available in Brainstorm (Baillet et al., 2001). Videos synchronised to
440 electrophysiological traces can also be imported and visualized simultaneously in synchrony, for
441 marking behavioral events.

442 The software is supported by an expansive online documentation (with tutorial data) and online
443 user forum.

444

A tool for augmented research productivity and reproducibility

445

446 With IN-Brainstorm, electrophysiologists are provided a free, integrated software environment
447 that promotes and facilitates harmonized principles of data management, methods,
448 documentation, code verification and reproducibility of data analyses. Such practical and user-
449 friendly tools also accelerate the education of electrophysiologist trainees and promotes the
450 adoption and expansion of data harmonization efforts, such as BIDS and *Neurodata Without*
451 *Borders*.

452 Every instance of data processing is logged, with the filenames of the data used and time stamps
453 of execution. These simple, yet powerful features document the provenance of data derivatives
454 and analysis results. Custom IN analysis pipelines assembled for elementary processing blocks of
455 the software's library can be shared with collaborators, publishers and the scientific community.
456 Pipelines are constructed via the GUI and saved as Matlab files. The open-source code of IN-
457 Brainstorm is thoroughly documented, verifiable and can benefit from contributions from any
458 user via GitHub. Sharing is further encouraged and facilitated by Brainstorm's data organization
459 in Studies, which can be zipped for archiving, exportation (e.g., as a BIDS repository) or
460 importation into the Brainstorm environment of a collaborator. Batch processing of multiple data
461 volumes is automated, thanks to the systematic organization of Brainstorm's file system and can
462 be executed on high-performance computing servers without requiring GUI interactions.

463 For all these reasons, we believe that IN-Brainstorm responds to an unmet need of the
464 electrophysiology community. By providing a unique environment with a common set of
465 analytical tools, the application also provides a unique bridge between recording scales, data

466 types and researchers, and additionally, between the methods used in human, animal and slice
467 preparations. It also represents a scalable framework to developments and integration of existing
468 or future tools and data formats for the entire field of electrophysiology.

469

470

Acknowledgements

481

482

Competing Interests

484 No competing interests declared by the authors.

485

486

487

488

489

490

491

492

493

494

495

496

14

References

497   Abbott, L.F., and Dayan, P. (1999). The effect of correlated variability on the accuracy of a population code.
499   Neural Comput. *11*, 91–101.

500   Abraham, A., Pedregosa, F., Eickenberg, M., Gervais, P., Mueller, A., Kossaifi, J., Gramfort, A., Thirion, B.,
501   and Varoquaux, G. (2014). Machine learning for neuroimaging with scikit-learn. Front. Neuroinformatics
502   *8*.

503   Arce-McShane, F., Sessle, B.J., Ross, C.F., and Hatsopoulos, N.G. (2018). Primary sensorimotor cortex
504   exhibits complex dependencies of spike-field coherence on neuronal firing rates, field power, and
505   behavior. J. Neurophysiol.

506   Averbeck, B.B., Latham, P.E., and Pouget, A. (2006). Neural correlations, population coding and
507   computation. Nat. Rev. Neurosci. *7*, 358–366.

508   Baillet, S., Mosher, J.C., and Leahy, R.M. (2001). Electromagnetic brain mapping. IEEE Signal Process. Mag.
509   *18*, 14–30.

510   Baillet, S., Friston, K., and Oostenveld, R. (2011). Academic Software Applications for Electromagnetic
511   Brain Mapping Using MEG and EEG.

512   Baker, M. (2016). 1,500 scientists lift the lid on reproducibility. Nat. News *533*, 452.

513   Bell, A.J., and Sejnowski, T.J. (1995). An information-maximization approach to blind separation and blind
514   deconvolution. Neural Comput. *7*, 1129–1159.

515   Buzsáki, G. (2006). Rhythms of the Brain (Oxford University Press).

516   Canolty, R.T., Edwards, E., Dalal, S.S., Soltani, M., Nagarajan, S.S., Kirsch, H.E., Berger, M.S., Barbaro, N.M.,
517   and Knight, R.T. (2006). High Gamma Power Is Phase-Locked to Theta Oscillations in Human Neocortex.
518   Science *313*, 1626–1628.

519   Cardoso, J.F. (1999). High-order contrasts for independent component analysis. Neural Comput. *11*, 157–
520   192.

521   Cichy, R.M., Pantazis, D., and Oliva, A. (2014). Resolving human object recognition in space and time. Nat.
522   Neurosci. *17*, 455.

523   Cui, Y., Liu, L.D., McFarland, J.M., Pack, C.C., and Butts, D.A. (2016). Inferring Cortical Variability from Local
524   Field Potentials. J. Neurosci. Off. J. Soc. Neurosci. *36*, 4121–4135.

525   Dale, A.M., Fischl, B., and Sereno, M.I. (1999). Cortical Surface-Based Analysis: I. Segmentation and Surface
526   Reconstruction. NeuroImage *9*, 179–194.

527   Eyherabide, H.G., and Samengo, I. (2013). When and Why Noise Correlations Are Important in Neural
528   Decoding. J. Neurosci. *33*, 17921–17936.

529   Fee, M.S., Mitra, P.P., and Kleinfeld, D. (1996). Automatic sorting of multiple unit neuronal signals in the
530   presence of anisotropic and non-Gaussian variability. J. Neurosci. Methods *69*, 175–188.

531 Fischl, B., Liu, A., and Dale, A.M. (2001). Automated manifold surgery: constructing geometrically accurate
532 and topologically correct models of the human cerebral cortex. IEEE Trans. Med. Imaging *20*, 70–80.

533 Fries, P. (2005). A mechanism for cognitive dynamics: neuronal communication through neuronal
534 coherence. Trends Cogn. Sci. *9*, 474–480.

535 Fries, P., Reynolds, J.H., Rorie, A.E., and Desimone, R. (2001). Modulation of Oscillatory Neuronal
536 Synchronization by Selective Visual Attention. Science *291*, 1560–1563.

537 Fries, P., Schröder, J.-H., Roelfsema, P.R., Singer, W., and Engel, A.K. (2002). Oscillatory neuronal
538 synchronization in primary visual cortex as a correlate of stimulus selection. J. Neurosci. Off. J. Soc.
539 Neurosci. *22*, 3739–3754.

540 Fries, P., Womelsdorf, T., Oostenveld, R., and Desimone, R. (2008). The Effects of Visual Stimulation and
541 Selective Visual Attention on Rhythmic Neuronal Synchronization in Macaque Area V4. J. Neurosci. *28*,
542 4823–4835.

543 Gorgolewski, K.J., and Poldrack, R.A. (2016). A Practical Guide for Improving Transparency and
544 Reproducibility in Neuroimaging Research. PLOS Biol. *14*, e1002506.

545 Gorgolewski, K., Burns, C.D., Madison, C., Clark, D., Halchenko, Y.O., Waskom, M.L., and Ghosh, S.S. (2011).
546 Nipype: A Flexible, Lightweight and Extensible Neuroimaging Data Processing Framework in Python. Front.
547 Neuroinformatics *5*.

548 Gorgolewski, K.J., Auer, T., Calhoun, V.D., Craddock, R.C., Das, S., Duff, E.P., Flandin, G., Ghosh, S.S.,
549 Glatard, T., Halchenko, Y.O., et al. (2016). The brain imaging data structure, a format for organizing and
550 describing outputs of neuroimaging experiments. Sci. Data *3*, 160044.

551 Gramfort, A., Papadopoulo, T., Olivi, E., and Clerc, M. (2010). OpenMEEG: opensource software for
552 quasistatic bioelectromagnetics. Biomed. Eng. OnLine *9*, 45.

553 Gramfort, A., Luessi, M., Larson, E., Engemann, D.A., Strohmeier, D., Brodbeck, C., Goj, R., Jas, M., Brooks,
554 T., Parkkonen, L., et al. (2013). MEG and EEG data analysis with MNE-Python. Front. Neurosci. *7*.

555 Gramfort, A., Luessi, M., Larson, E., Engemann, D.A., Strohmeier, D., Brodbeck, C., Parkkonen, L., and
556 Hämäläinen, M.S. (2014). MNE software for processing MEG and EEG data. NeuroImage *86*, 446–460.

557 Gregoriou, G.G., Gotts, S.J., Zhou, H., and Desimone, R. (2009). High-Frequency, Long-Range Coupling
558 Between Prefrontal and Visual Cortex During Attention. Science *324*, 1207–1210.

559 Hanke, M., Halchenko, Y.O., Sederberg, P.B., Olivetti, E., Fründ, I., Rieger, J.W., Herrmann, C.S., Haxby, J.V.,
560 Hanson, S.J., and Pollmann, S. (2009). PyMVPA: a unifying approach to the analysis of neuroscientific data.
561 Front. Neuroinformatics *3*.

562 Hazan, L., Zugaro, M., and Buzsáki, G. (2006). Klusters, NeuroScope, NDManager: a free software suite for
563 neurophysiological data processing and visualization. J. Neurosci. Methods *155*, 207–216.

564 Hill, D.N., Mehta, S.B., and Kleinfeld, D. (2011). Quality metrics to accompany spike sorting of extracellular
565 signals. J. Neurosci. Off. J. Soc. Neurosci. *31*, 8699–8705.

566   Holdgraf, C., Appelhoff, S., Bickel, S., Bouchard, K., D'Ambrosio, S., David, O., Devinsky, O., Dichter, B.,
567   flinker, adeen, Foster, B., et al. BIDS-iEEG: an extension to the brain imaging data structure (BIDS)
568   specification for human intracranial electrophysiology.

569   Jin, J.Z., Weng, C., Yeh, C.-I., Gordon, J.A., Ruthazer, E.S., Stryker, M.P., Swadlow, H.A., and Alonso, J.-M.
570   (2008). On and off domains of geniculate afferents in cat primary visual cortex. Nat. Neurosci. *11*, 88–94.

571   Krause, M.R., Zanos, T.P., Csorba, B.A., Pilly, P.K., Choe, J., Phillips, M.E., Datta, A., and Pack, C.C. (2017).
572   Transcranial Direct Current Stimulation Facilitates Associative Learning and Alters Functional Connectivity
573   in the Primate Brain. Curr. Biol. *27*, 3086-3096.e3.

574   Kybic, J., Clerc, M., Abboud, T., Faugeras, O., Keriven, R., and Papadopoulo, T. (2005). A common formalism
575   for the Integral formulations of the forward EEG problem. IEEE Trans. Med. Imaging *24*, 12–28.

576   Larson, M.J., and Moser, J.S. (2017). Rigor and replication: Toward improved best practices in human
577   electrophysiology research. Int. J. Psychophysiol. *111*, 1–4.

578   Legatt, A.D., Arezzo, J., and Vaughan, H.G. (1980). Averaged multiple unit activity as an estimate of phasic
579   changes in local neuronal activity: effects of volume-conducted potentials. J. Neurosci. Methods *2*, 203–
580   217.

581   Liebe, S., Hoerzer, G.M., Logothetis, N.K., and Rainer, G. (2012). Theta coupling between V4 and prefrontal
582   cortex predicts visual short-term memory performance. Nat. Neurosci. *15*, 456–462.

583   Liu, L.D., Haefner, R.M., and Pack, C.C. A neural basis for the spatial suppression of visual motion
584   perception. ELife *5*.

585   Mineault, P.J., Zanos, T.P., and Pack, C.C. (2013). Local field potentials reflect multiple spatial scales in V4.
586   Front. Comput. Neurosci. *7*, 21.

587   Mitra, P., and Bokil, H. (2007). Observed Brain Dynamics (Oxford ; New York: Oxford University Press).

588   Nauhaus, I., Busse, L., Carandini, M., and Ringach, D.L. (2009). Stimulus contrast modulates functional
589   connectivity in visual cortex. Nat. Neurosci. *12*, 70–76.

590   Niso, G., Rogers, C., Moreau, J.T., Chen, L.-Y., Madjar, C., Das, S., Bock, E., Tadel, F., Evans, A.C., Jolicoeur,
591   P., et al. (2016). OMEGA: The Open MEG Archive. NeuroImage *124*, 1182–1187.

592   Oostenveld, R., Fries, P., Maris, E., and Schoffelen, J.-M. (2011). FieldTrip: Open Source Software for
593   Advanced Analysis of MEG, EEG, and Invasive Electrophysiological Data.

594   Pachitariu, M., Steinmetz, N.A., Kadir, S.N., Carandini, M., and Harris, K.D. (2016). Fast and accurate spike
595   sorting of high-channel count probes with KiloSort. In Advances in Neural Information Processing Systems
596   29, D.D. Lee, M. Sugiyama, U.V. Luxburg, I. Guyon, and R. Garnett, eds. (Curran Associates, Inc.), pp. 4448–
597   4456.

598   Panzeri, S., Schultz, S.R., Treves, A., and Rolls, E.T. (1999). Correlations and the encoding of information in
599   the nervous system. Proc. R. Soc. B Biol. Sci. *266*, 1001–1012.

600   Pernet, C.R., Appelhoff, S., Flandin, G., Phillips, C., Delorme, A., and Oostenveld, R. BIDS-EEG: an extension
601   to the Brain Imaging Data Structure (BIDS) Specification for electroencephalography.

602   Pesaran, B., Pezaris, J.S., Sahani, M., Mitra, P.P., and Andersen, R.A. (2002). Temporal structure in neuronal
603   activity during working memory in macaque parietal cortex. Nat. Neurosci. *5*, 805–811.

604   Quiroga, R.Q. (2007). Spike sorting. Scholarpedia *2*, 3583.

605   Quiroga, R.Q., Nadasdy, Z., and Ben-Shaul, Y. (2004). Unsupervised Spike Detection and Sorting with
606   Wavelets and Superparamagnetic Clustering. Neural Comput. *16*, 1661–1687.

607   Ray, S., and Maunsell, J.H.R. (2011). Network Rhythms Influence the Relationship between Spike-
608   Triggered Local Field Potential and Functional Connectivity. J. Neurosci. *31*, 12674–12682.

609   Shattuck, D.W., and Leahy, R.M. (2002). Brainsuite: An automated cortical surface identification tool. Med
610   Image Anal *6*, 129–142.

611   Singer, W. (1999). Neuronal Synchrony: A Versatile Code for the Definition of Relations? Neuron *24*, 49–
612   65.

613   Sompolinsky, H., Yoon, H., Kang, K., and Shamir, M. (2001). Population coding in neuronal systems with
614   correlated noise. Phys. Rev. E Stat. Nonlin. Soft Matter Phys. *64*, 051904.

615   Stead, M., and Halford, J.J. (2016). A Proposal for a Standard Format for Neurophysiology Data Recording
616   and Exchange. J. Clin. Neurophysiol. Off. Publ. Am. Electroencephalogr. Soc. *33*, 403–413.

617   Tadel, F., Baillet, S., Mosher, J.C., Pantazis, D., and Leahy, R.M. (2011). Brainstorm: A User-Friendly
618   Application for MEG/EEG Analysis, Brainstorm: A User-Friendly Application for MEG/EEG Analysis.
619   Comput. Intell. Neurosci. Comput. Intell. Neurosci. *2011*, *2011*, e879716.

620   Teeters, J.L., Godfrey, K., Young, R., Dang, C., Friedsam, C., Wark, B., Asari, H., Peron, S., Li, N., Peyrache,
621   A., et al. (2015). Neurodata Without Borders: Creating a Common Data Format for Neurophysiology.
622   Neuron *88*, 629–634.

623   Uusitalo, M.A., and Ilmoniemi, R.J. (1997). Signal-space projection method for separating MEG or EEG into
624   components. Med. Biol. Eng. Comput. *35*, 135–140.

625   Wilke, M., Logothetis, N.K., and Leopold, D.A. (2006). Local field potential reflects perceptual suppression
626   in monkey visual cortex. Proc. Natl. Acad. Sci. *103*, 17507–17512.

627   Womelsdorf, T., Fries, P., Mitra, P.P., and Desimone, R. (2006). Gamma-band synchronization in visual
628   cortex predicts speed of change detection. Nature *439*, 733–736.

629   Womelsdorf, T., Schoffelen, J.-M., Oostenveld, R., Singer, W., Desimone, R., Engel, A.K., and Fries, P.
630   (2007). Modulation of Neuronal Interactions Through Neuronal Synchronization. Science *316*, 1609–1612.

631   Zanos, T.P., Mineault, P.J., and Pack, C.C. (2011). Removal of Spurious Correlations Between Spikes and
632   Local Field Potentials. J. Neurophysiol. *105*, 474–486.

633   Zohary, E., Shadlen, M.N., and Newsome, W.T. (1994). Correlated neuronal discharge rate and its
634   implications for psychophysical performance. Nature *370*, 140–143.

635

Figures
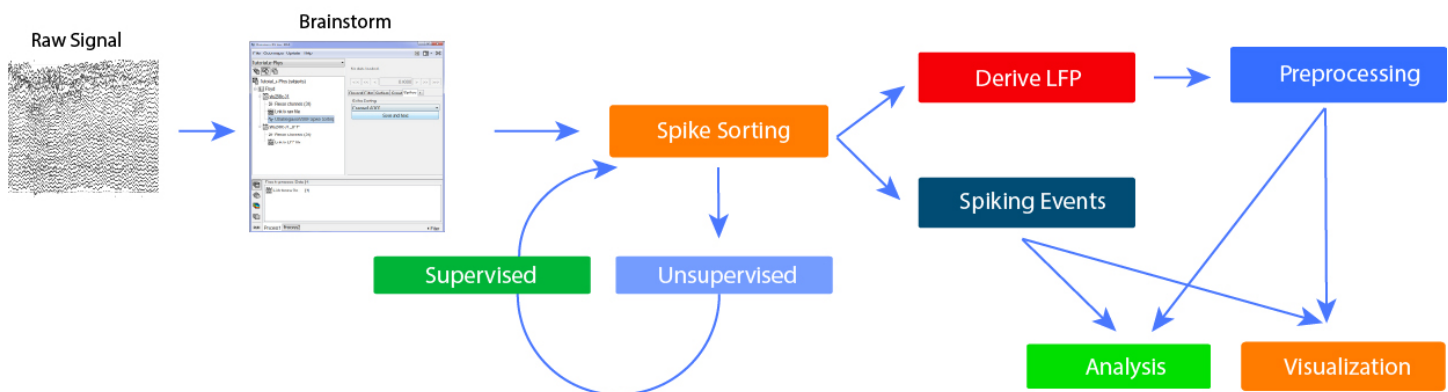
Figure 1. Workflow of the toolbox

Figure 1. Workflow of the e-Phys toolbox. Users initially import the header to the raw binary signal. Once the data is identified, the users perform the spike-sorting step. The spike-sorting process is divided into two parts: Unsupervised (the algorithm creates neuronal clusters automatically) and Supervised (the user inspects the output of the unsupervised part). At this point of the workflow, the LFP can be extracted. All the spiking events that were previously computed and the down-sampled LFP signals are all encapsulated to a single binary file. The original binary file can be stored to an external source and is no-longer needed. Finally, users can now perform preprocessing and analyze their data, utilizing the spike-related function that have been introduced to Brainstorm by this toolbox.

e-PHYS TOOLBOX	
Acquisition Systems	Blackrock (.nsX), Ripple (.nsX), Plexon (.plx, .pl2), Intan (.rhd), Neurodata without borders (.nwb), Tucker Davis Technologies
Spike Sorters	WaveClus, UltraMegaSort2000, Kilosort (Klusters)
LFP spectral Artifact Removal	Bayesian spectral spiking-artifact removal
Spike-related Functions	Tuning Curves, Raster Plots, Spike Field Coherence, Spike triggered Average
LFP - ANALYSIS	
Pre-processing	DC-offset removal, Band-pass / band-stop / notch filtering, resampling
Artifact Removal	SSP, ICA
Frequency	FFT, Welch Density, Morlet Wavelets, Hilbert transform, Multi-tapers, Phase Amplitude Coupling, Instantaneous frequency, Canolty Maps
Connectivity	Correlation, coherence, Bivariate Granger causality, Phase Locking Value, Amplitude Envelope Correlation, Phase Transfer Entropy
Statistics and machine learning	Parametric testing (zero / baseline), Partial Least Squares, Support Vector Machine classification, Linear Discriminant Analysis classification

Table 1. Synopsis of the e-Phys toolbox and the tools that can be used for LFP analysis. The e-Phys toolbox provides a working framework for every step of the e-Phys analysis and each module can easily be enriched with future additions.

Figure 2. Dataset navigation and pre-processing window
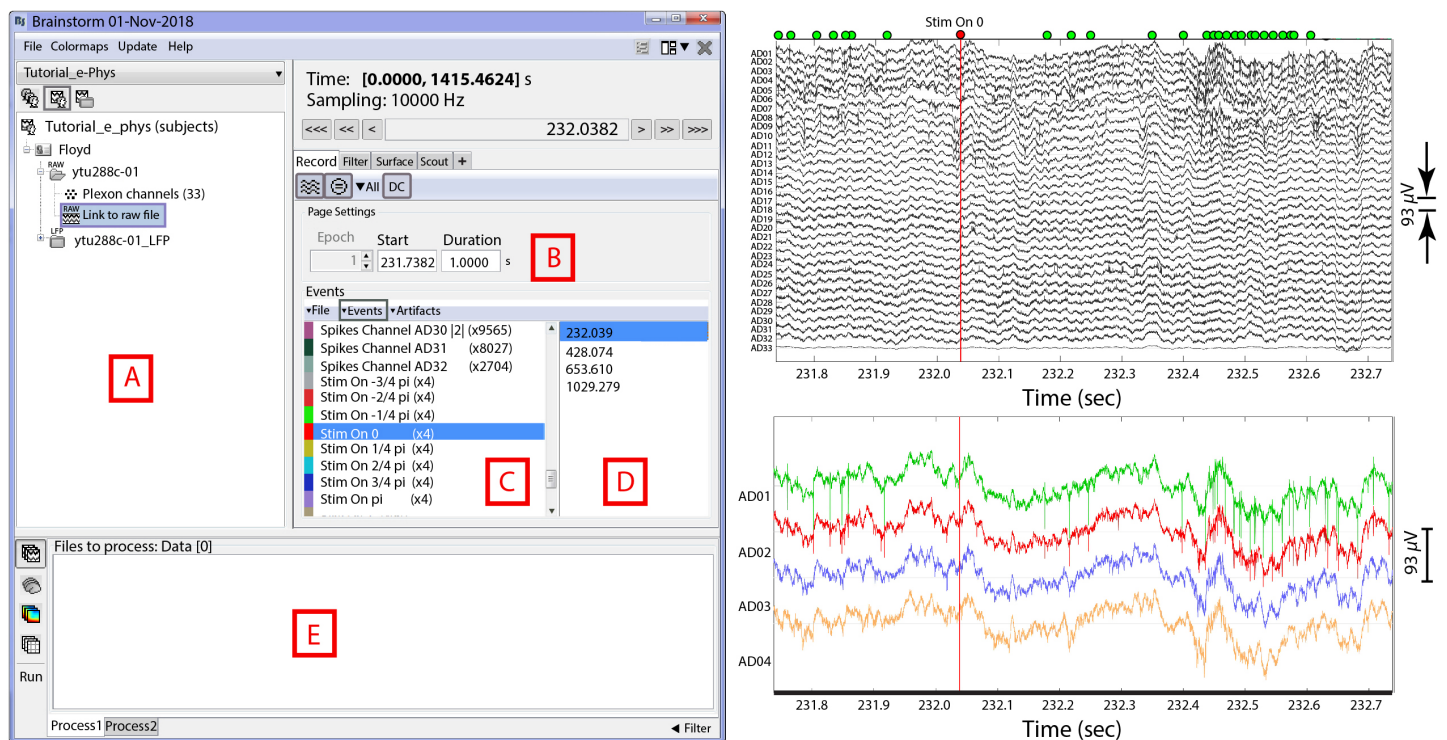
Figure 2. Left: (A) Main Brainstorm window showing the created dataset entry (ytu288c-01) on the data-tree section. (B) Selection of starting time point and duration of signal segment to be loaded for reviewing. (C) Experimental and spiking events are displayed. (D) An event is selected from the "Stim on 0" condition. This selection automatically synchronizes all reviewing windows to the timepoint of the event's occurrence. Right Top: 1 second segment displaying raw signals from all electrodes. The vertical red line indicates alignment around the selected event ("Stim On 0"). The green dots on the top of the figure represent the spiking events from the first neuron on electrode with label AD01. Right Bottom: A selection of the first 4 electrodes, aligned in time with the top figure.

Figure 3. Unsupervised Spike-sorting
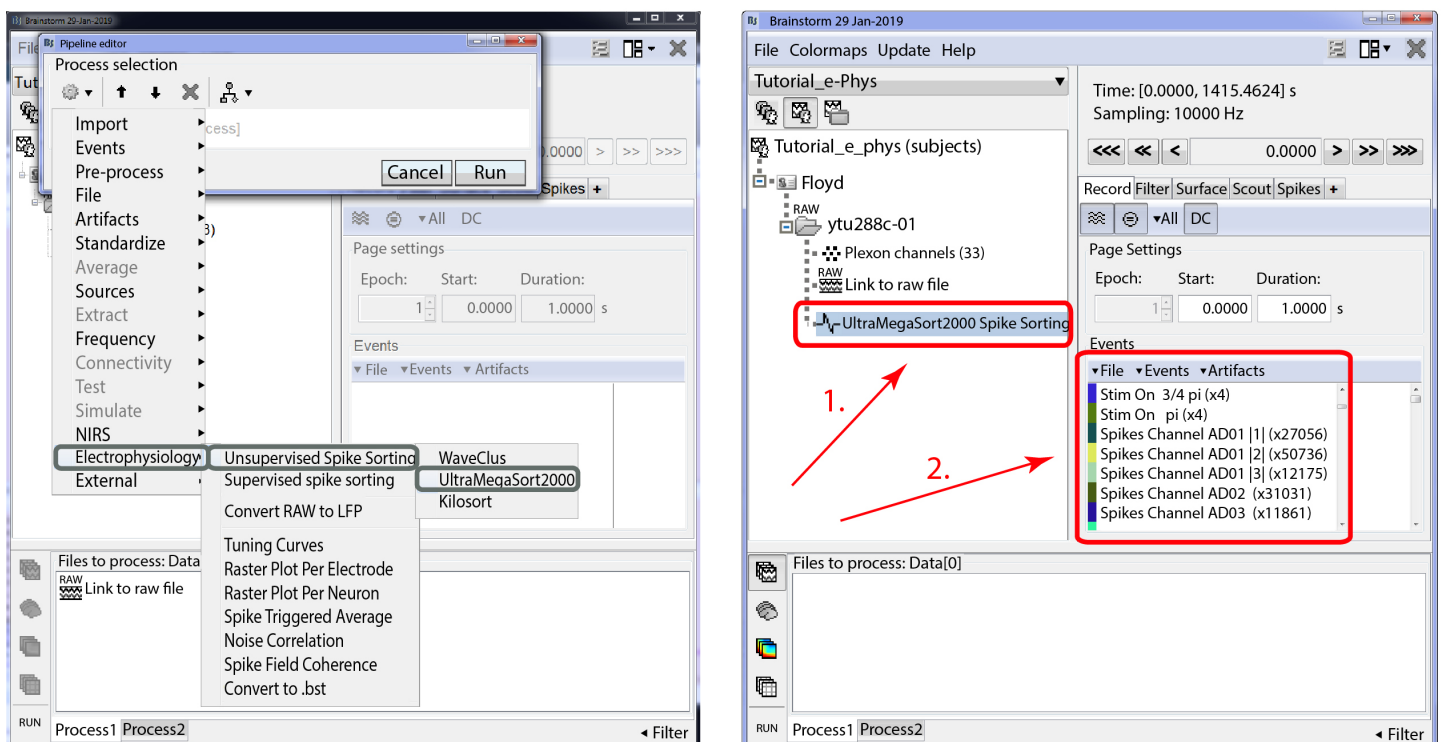
Figure 3. Left: Selection of the embedded spike-sorters for unsupervised spike-sorting within Brainstorm. Right: Example of a dataset spike-sorted with UltraMegaSort2000. (Box 1)A new entry in the database UltraMegaSort2000 Spike Sorting appears and indicates that this dataset has been spike-sorted. (Box 2). New events appear in the Events window, corresponding to the spikes that the spike-sorter clustered (Spikes Channel X).
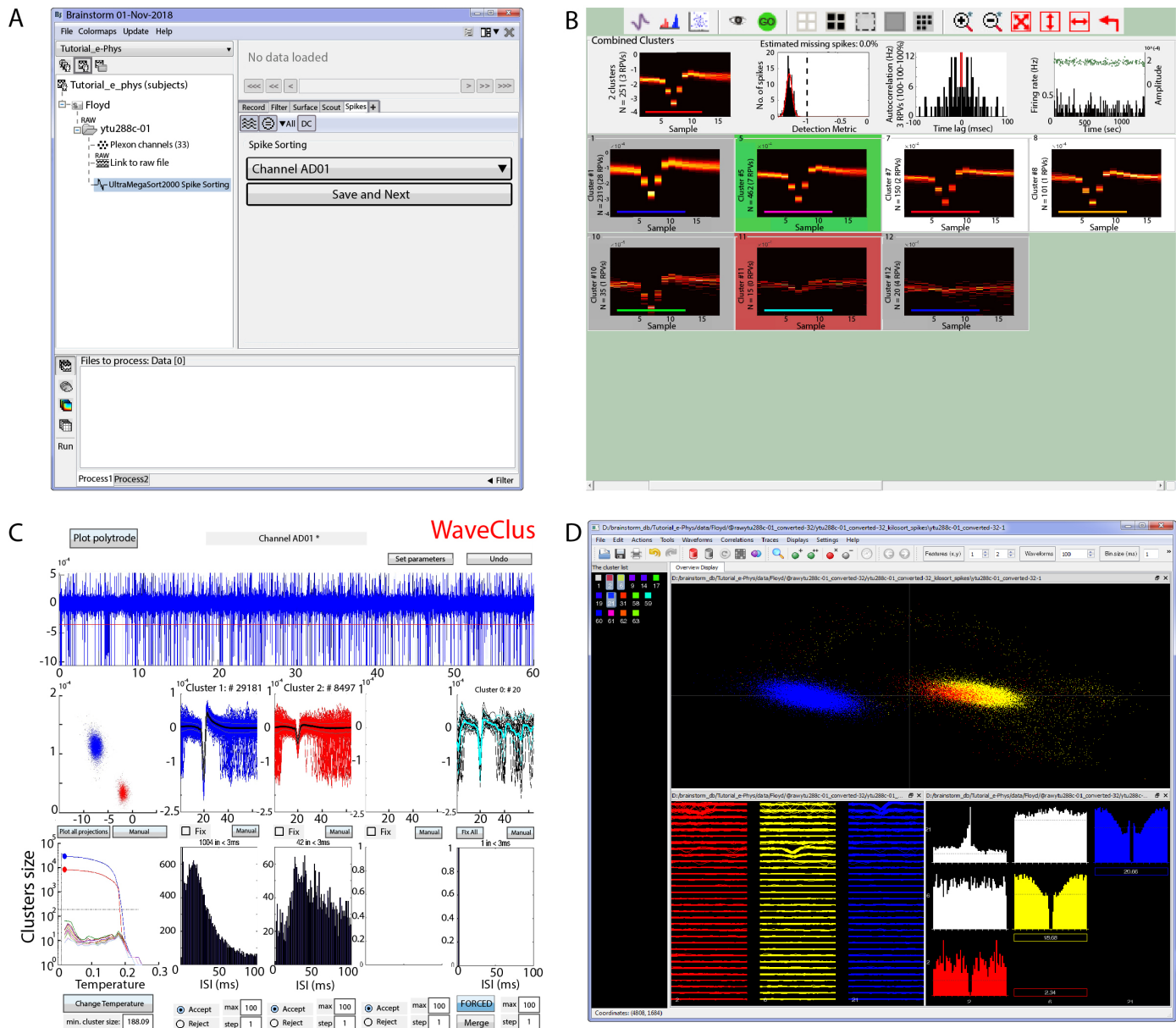
Figure 4. Supervised spike-sorting

Figure 4. Supervised spike sorting. (A). Main window that the user selects the electrode (or group of electrodes for Klusters) and the spike sorted files automatically update the spike sorter in use. Once the neuronal clusters have been adjusted, the user presses the Save and Next button and the next electrode gets selected to continue the supervised spike-sorting. (B, C, D). Supervised GUI for UltraMegaSort, WaveClus and Klusters respectively.

Figure 5. Conversion from raw signals to LFPs
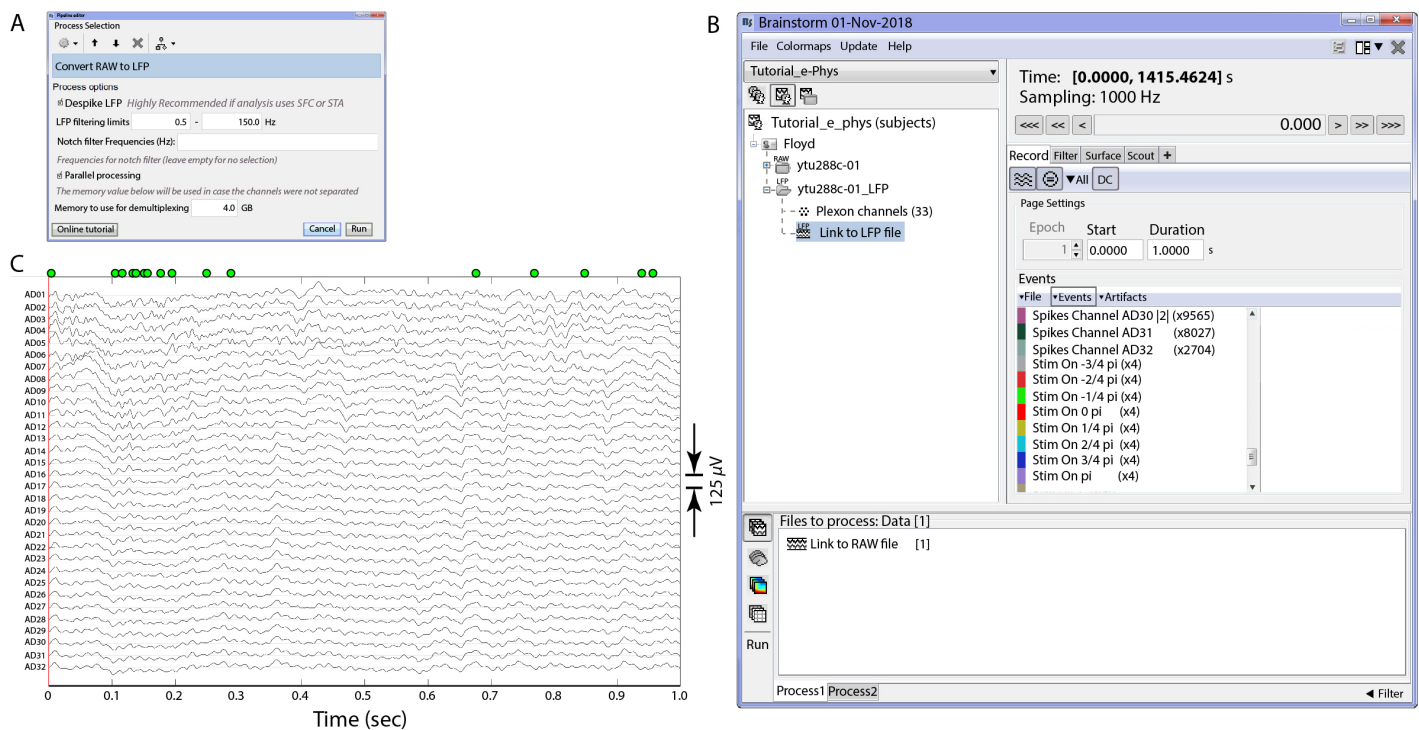
Figure 5. Converter from raw signals to LFPs. (A). Users can select the filtering limits of their LFP and apply a notch filter if necessary. The converter downsamples the raw signal to 1 KHz. (B). Once the conversion is complete, a single binary file (.bst) that contains all the necessary information (LFPs, experimental and spiking events) is stored on the hard drive, and automatically imported on the data-tree as a new dataset. (C). 1 second segment review of the created LFP signal traces. The spiking events from the first neuron of electrode AD01 are represented by the green dots on the top of the figure, as in Figure 2.
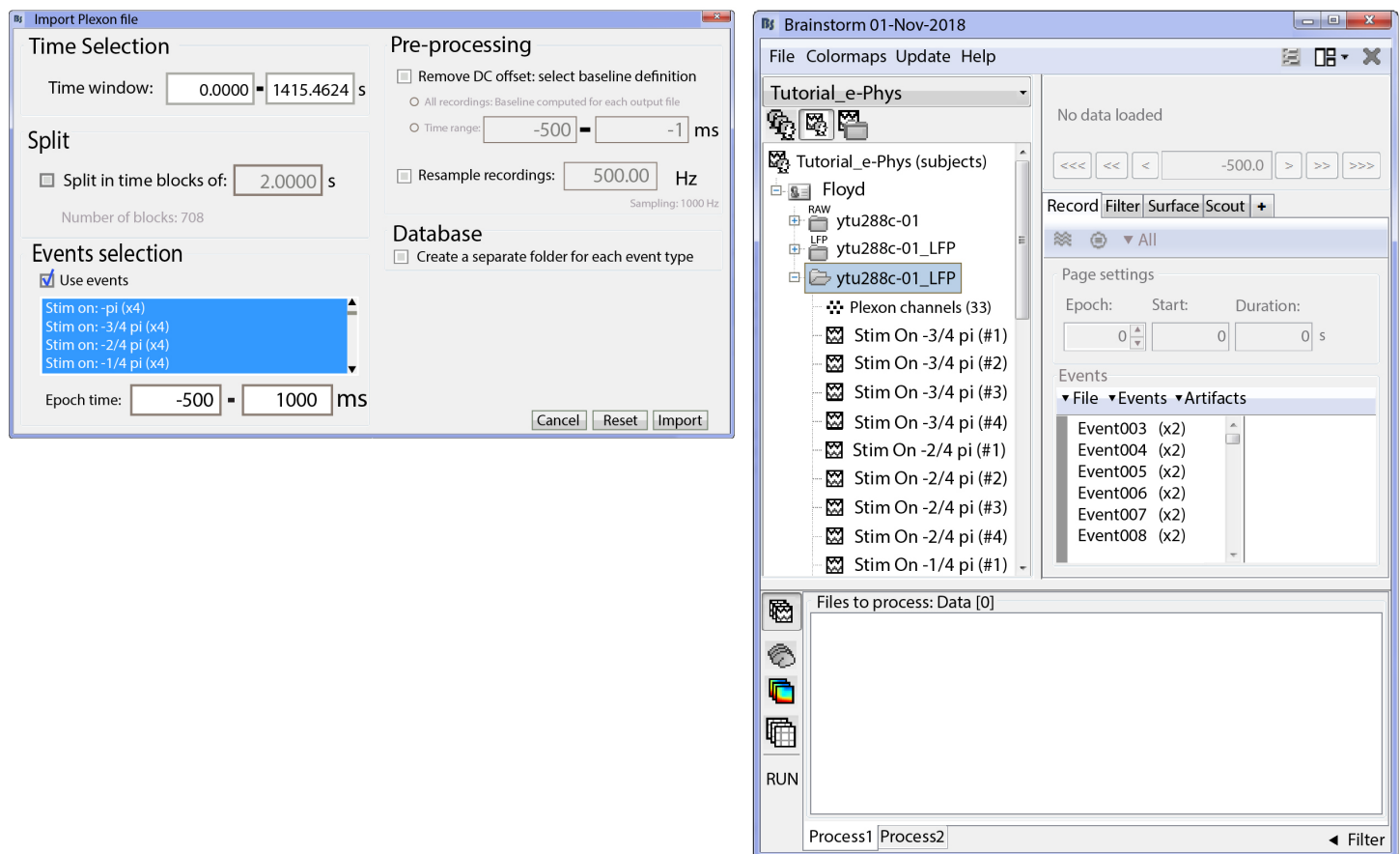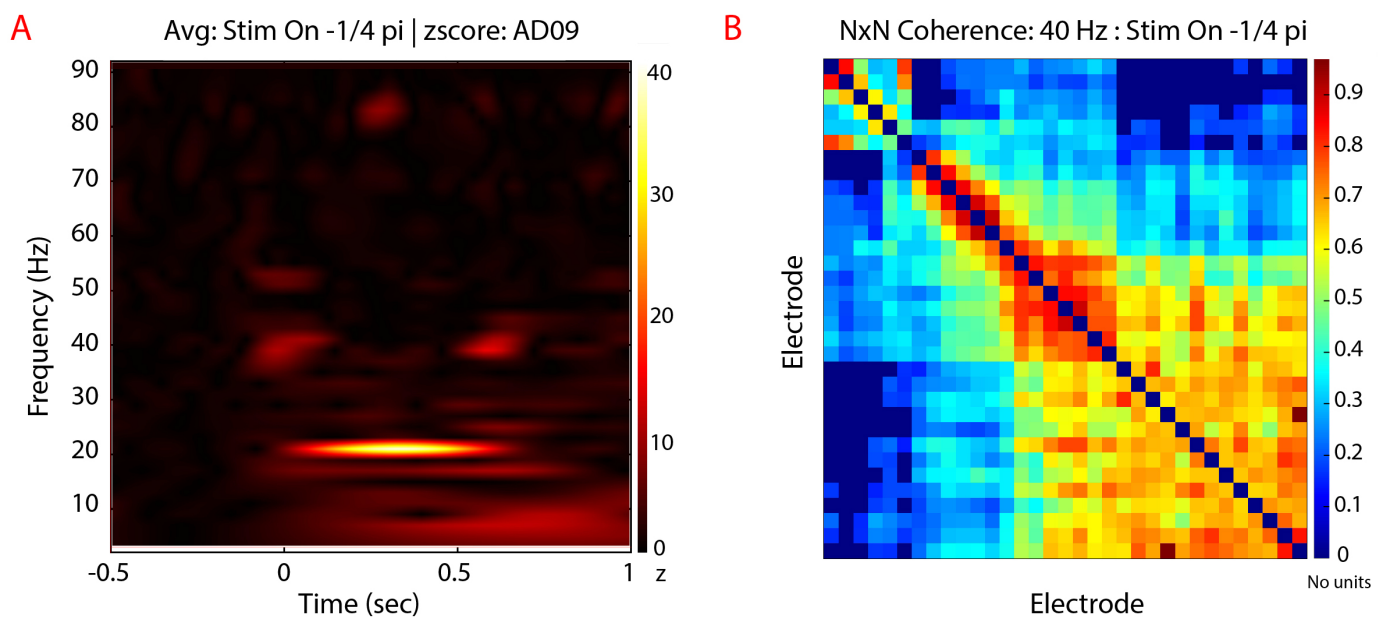
Figure 6. Importing of trials

Figure 6. (Left) Selection of the events of interest and temporal boundaries around them, for importing the LFP segments. (Right) Imported LFP trials for the selected conditions in the Brainstorm database.

Figure 7. Analysis of LFP signals

Figure 7. (A). Wavelet Decomposition ([2-90] Hz) of a single LFP trial from electrode labeled AD09 for moving stimulus condition towards -1/4 pi degrees direction. Users can select the channel they want to be displayed from a drop-down list on the main Brainstorm window.

(B). Estimation of NxN coherence for a single trial across all electrodes. The coherence values are color-coded for a specific frequency (on the example 40 Hz frequency is selected). Users can display coherence in the other frequencies by moving a sliding toggle.

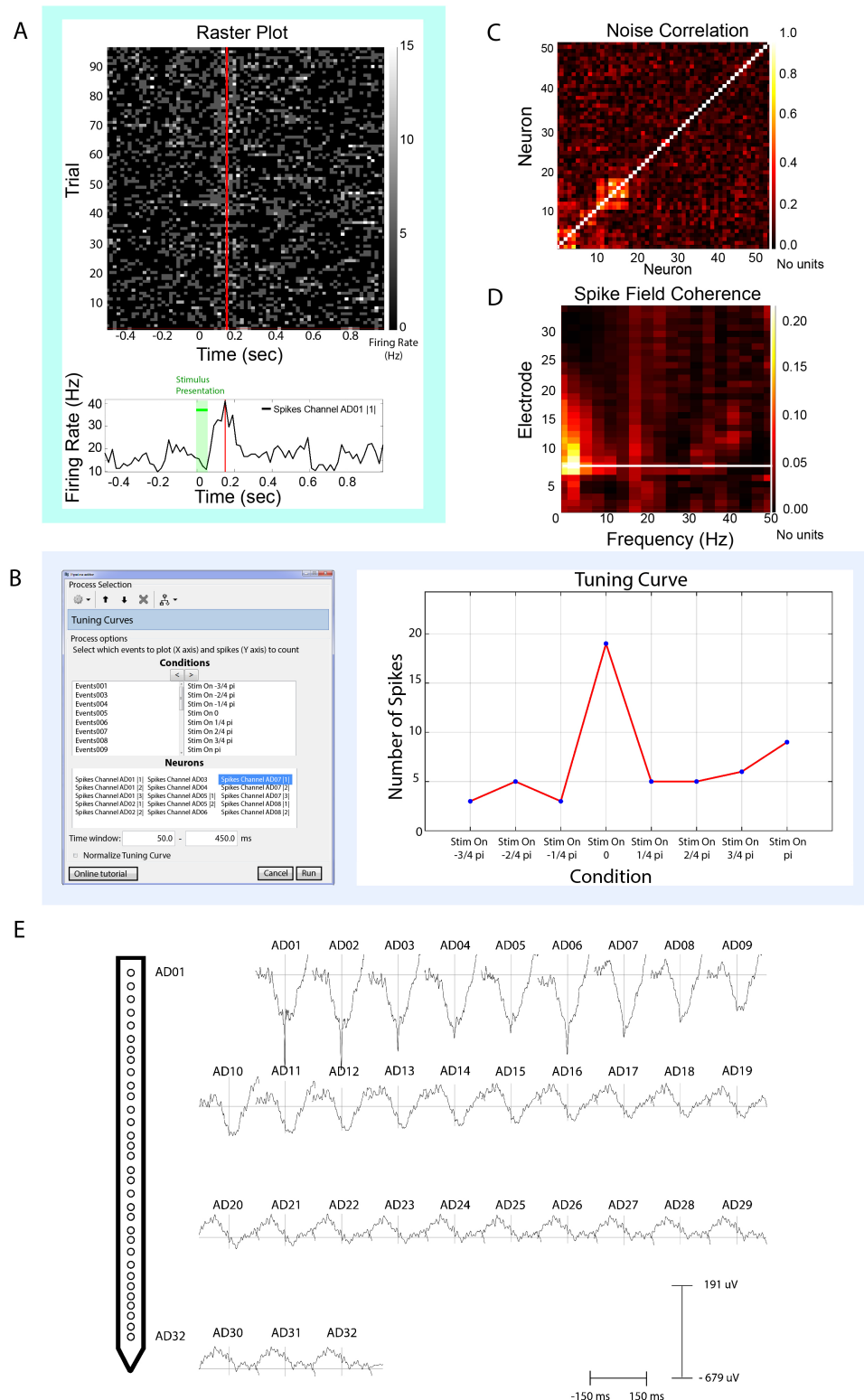## Figure 8. Spike-LFP analysis functions

Figure 8. (A) Raster Plot. (Top) Example raster plot for 96 trials of a single condition for the first neuron picked up on electrode labeled 'AD01'. Firing has been binned into 10ms segments. The green shading indicates the period where the stimulus was presented on the screen. A single condition was repeated 96 times instead of 4 for the purpose of this raster plot. (Bottom) Average firing rate from all trials shows maximum firing ~150ms after the stimulus onset for this neuron. The vertical red line indicates interactive temporal alignment between the two plots and the green shade the period of the stimulus presentation.

(B) Tuning curves function. (LEFT): Users select the neurons that they want to display the tuning curves, and sequentially the conditions (and their order) that would formulate the x-axis (right side of the conditions selection window). Additionally, we included a selection for the time-window where the spikes would be counted. (RIGHT): Tuning curve for an example neuron, selected from the window on the left of Figure B. The x-axis shows the different experimental conditions at the order selected on the previous window. This neuron expresses selectivity for the condition "Stim On 0".

(C) Noise correlation. The function selects all the neurons that elicited spikes within the trials imported and displays a nxn figure where the noise correlation is computed for all combinations of neurons. Specifically for the dataset illustrated, there were 53 unique neurons picked up by the electrodes (according to the spike sorting step). This figure shows the computation of noise-correlation on all trials (a subset on a specific condition is also possible) for the presentation 96 trials of a motion stimulus, and spikes are selected on [0,300] ms around the stimuli presentations.

(D) Spike field coherence for an example neuron picked up from the first electrode (AD07) for the motion stimulus condition "Stim On 0". The spike-field coherence window displays spectral influence of a single neuron to all 32 electrodes. Frequency is shown up to 60 Hz. Time selection around each spike was [-150, 150] ms

(E) Spike triggered average of a neuron picked up on electrode labeled AD01. A graph of the linear probe with the relative electrode locations is displayed on the left of the figure. The time selection around the spikes was set to [-150,150] ms for all trials of all experimental conditions. The electrodes have been presented into four rows for easier visualization. In reality, the linear probe extends on a single dimension (1:32). The scale of the STA is shown on the bottom right. All traces have been aligned to the same time-selection (0 ms – time occurrence of the spikes of AD01), indicated by the vertical line of each signal's display.

Figure 9. Topographical visualizations
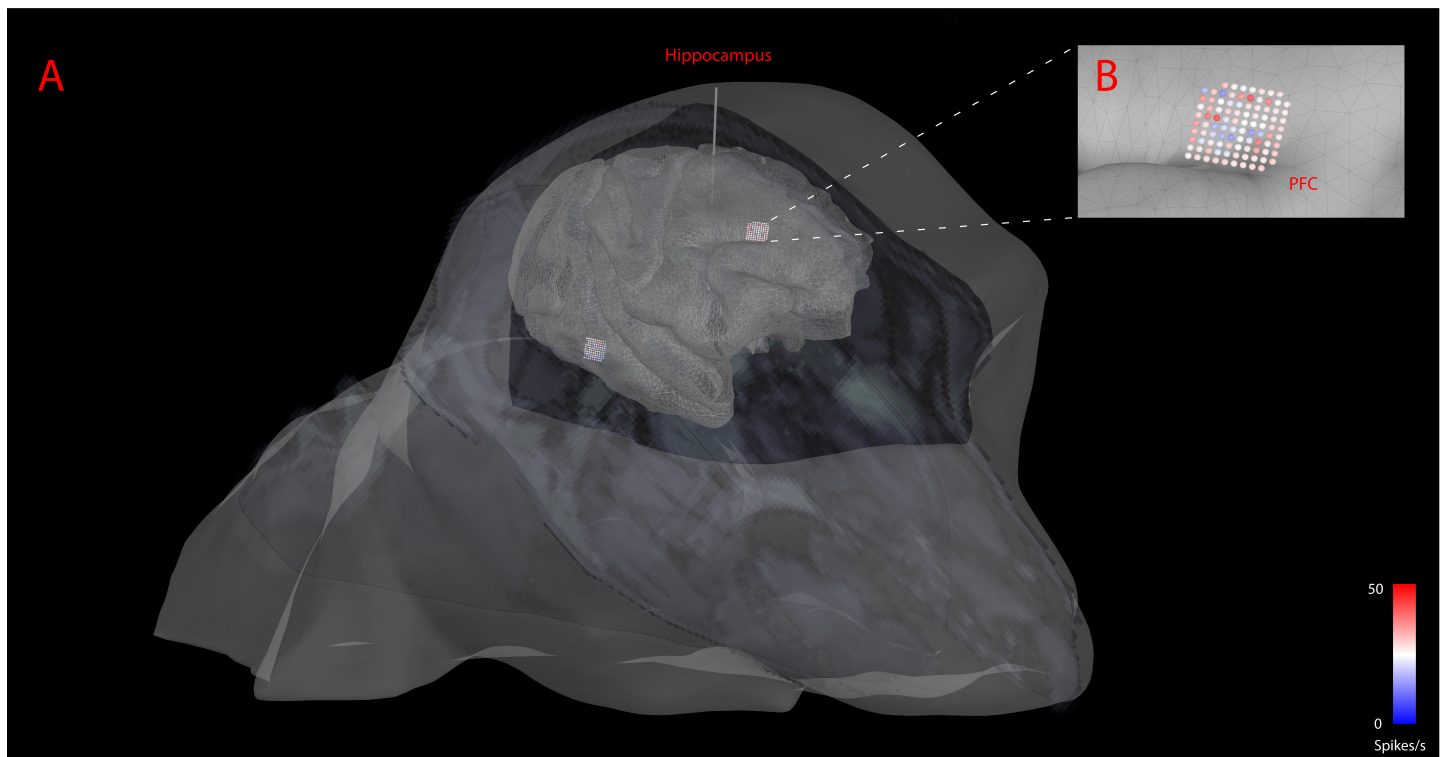
Figure 9. (A). Visualization of the implanted electrodes on the anatomical MRI of the non-human primate. The MR slices are superimposed on the figure. (B). Zoomed in version of an implanted Utah array on the cortical surface, with the spiking activity color-coded on the array's topography for a single time-bin.